PHYSICAL REVIEW B VOLUME 3, NUMBER 6 15 MARCH 1971

Simplified Theory of Electron Correlations in Metals

A. W. Overhauser
Scientific Research Staff, Ford Motor Company, Dearborn, Michigan 48121
(Received 21 September 1970)

A model is developed which allows one to easily calculate correlation effects of interacting electrons. Upon considering a particular electron one replaces the excitation spectrum of all other electrons by a single mode $\omega(q)$, varying between the plasma frequency for small q and $\hbar q^2/2m$ for large q. The coupling strength between the electron and the plasma modes is found by imposing the f sum rule. $\omega(q)$ is determined by requiring the model to have a correct dielectric response. The exchange and correlation contributions to $E(k)$ have nearly opposite k dependence. However, there is a residual oscillation near k_F which causes the effective mass m^* to be less than unity, even though the mean mass (between $k=0$ and k_F) is greater than unity. A specific local approximation to the exchange and correlation potential $A_{xc} = -2.07(na_0^3)^{0.3}$ Ry, analogous to Slater's $n^{1/3}$ exchange potential, is accurate over 3 orders of magnitude in density. The (bare) momentum distribution $n(k)$, and the fraction ζ of electrons excited above k_F, are calculated as a function of density. For Li and Na, excluding band-structure effects, $\zeta = 0.11$ and 0.14, respectively.

I. INTRODUCTION

During the last twenty years there have been many calculations of the correlation energy of a degenerate electron gas. There is hardly need for another. Instead, the object of this study is to develop a simplified model for treating correlations which can be easily applied to complex problems. Accordingly, our attention is focused on the behavior of individual electrons, the contribution of correlation to one-electron energy spectra, and the dynamical effects of correlation when electrons experience nonuniform perturbations (caused by interaction with periodic potentials, phonons, photons, magnons, etc.). These latter applications, however, will be left for subsequent development.

The model proposed is just that – a model, and necessarily depends on approximation and oversimplification of reality. Its limitations must be kept in mind. Nevertheless, it is intended that it be physically motivated and transparent, that it have *a priori* appeal, and that it be, moreover, as accurate as possible. In this regard, the recent work of Singwi *et al.*[1] (SSTL) is selected as a guide.

Attention is focused on an individual test charge or electron imbedded in a degenerate electron gas. The electron gas will be regarded as a dielectric medium. Interaction of the particle with the medium is determined by the excitation spectrum of the medium. Generally, there are two types of excitation for a given wave-vector transfer $\vec{q}$: collective excitations (plasmons) and one-electron excitations. These are shown in Fig. 1. Plasmon excitations are most important for small q – indeed, they exhaust the f sum rule[2] – whereas one-electron excitations dominate exclusively for high q.

One reason why calculations incorporating correlation are so complex is that they involve summation over both types of excitation and, especially, the one-electron excitations require a double sum over momentum space. For very large q, the spectral width of the one-electron excitations becomes small compared to $\hbar^2q^2/2m$. In this limit, therefore, it is reasonable to collapse the spectrum into a single mode with $\hbar\omega(q) \to \hbar^2q^2/2m$.

The fundamental approximation of our model is replacement of the complete excitation spectrum of Fig. 1 by a single plasmon branch $\hbar\omega(q)$. For small q, $\omega(q)$ approaches the plasma frequency, and for large q it approaches $\hbar q^2/2m$. For reasons already given this model compromises reality primarily in the intermediate-q range, where the spectral width of the one-electron excitations is comparable to $\hbar\omega(q)$.

Two important theoretical questions arise in developing the model explicitly: What is the interaction coefficient for the coupling of the test charge

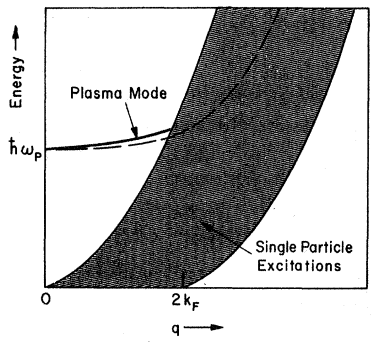

FIG. 1. Spectrum of excitation energies vs wave-vector transfer q for an interacting electron gas. Upper boundary of the single-particle excitations is $(\hbar^2/2m) \times[(k_F+q)^2-k_F^2]$, and lower boundary is $(\hbar^2/2m)[(-k_F+q)^2 - k_F^2]$. In the plasmon model, this spectrum is replaced by a single mode $\hbar\omega(q)$, indicated by the dashed line.

(or electron) to the plasmons, and what is the frequency spectrum $\omega(q)$? One might expect that specifying these functions involves some arbitrariness, but that is not the case. The interaction coefficient is determined unequivocally (for all q) by requiring fulfillment of the f sum rule; and $\omega(q)$ is fixed by requiring the model to reproduce the "correct" electron-gas dielectric function $\epsilon(q)$.

An advantage of the foregoing strategy, which we work out in detail below, is that the model is constrained to be accurate in several important physical aspects at the outset. However one may expect it to become unreliable, for example, in treating processes where the finite spectral width of the true excitation spectrum is crucial.

II. TEST-CHARGE-PLASMON INTERACTION

First, the interaction of a test charge (having charge $-e$) with the plasmons shall be considered, but specifying that it is not an electron. Thereby problems such as exchange are postponed to a later section.

The electron density $\rho(\vec{r})$ of the plasmon assembly, containing N electrons in a volume Ω, can be expanded in a Fourier series:

$$\rho(\vec{r}) \equiv \sum_{i=1}^{N} \delta(\vec{r} - \vec{r}_i) = \Omega^{-1} \sum_{\vec{q}} \rho_{\vec{q}}\, e^{-i\vec{q}\cdot\vec{r}} . \tag{1}$$

By Fourier inversion

$$\rho_{\vec{q}} = \sum_{i=1}^{N} e^{i\vec{q}\cdot\vec{r}_i} . \tag{2}$$

From Poisson's equation, the interaction Hamiltonian between a test charge (at $\vec{r}$) and the plasma is found to be

$$H'(\vec{r}) = \textstyle\sum_{\vec{q}} (4\pi e^2/q^2\Omega)\rho_{\vec{q}}\, e^{-i\vec{q}\cdot\vec{r}} . \tag{3}$$

The foregoing expression is not yet in the form we need, for $H'(\vec{r})$ is wanted in terms of the plasmon creation and annihilation operators $a_{\vec{q}}^{\dagger}$ and $a_{\vec{q}}$. $\rho(\vec{r})$ is anticipated to be related linearly as

$$\rho(\vec{r}) = \textstyle\sum_{\vec{q}} \lambda_q (a_{\vec{q}}\, e^{i\vec{q}\cdot\vec{r}} + a_{\vec{q}}^{\dagger} e^{-i\vec{q}\cdot\vec{r}}) , \tag{4}$$

where the coefficient $\lambda_q = \lambda(|\vec{q}|)$ is real. By changing $\vec{q} \to -\vec{q}$ in the first term of (4) and comparing with (1), it is found that

$$\rho_{\vec{q}} = \Omega\lambda_q (a_{-\vec{q}} + a_{\vec{q}}^{\dagger}) . \tag{5}$$

The coefficient λ_q needs to be determined. This is done by applying the f sum rule.

The f sum rule for an electron gas is derived[3] by evaluating the double commutator $[[H, \rho_{\vec{q}}], \rho_{\vec{q}}^{\dagger}]$, where H is the exact Hamiltonian $\sum (p_i^2/2m + V_{ij})$. One obtains[3]

$$\textstyle\sum_n \hbar\omega_{n0} \left| (\rho_{\vec{q}})_{n0} \right|^2 = N\hbar^2 q^2/2m . \tag{6}$$

$\{\hbar\omega_{n0}\}$ are the energy differences between the (exact) excited states $\{n\}$ and the ground state. Since the plasmon model assumes there is only one excitable mode for a given $\vec{q}$, all the oscillator strength must be concentrated in that mode. Accordingly, there would be just one term in the sum which, after substituting (5), reduces to

$$\hbar\omega_q \Omega^2 \lambda_q^2 = N\hbar^2 q^2/2m . \tag{7}$$

The well-known matrix elements (0 and 1) of $a_{\vec{q}}$ and $a_{\vec{q}}^{\dagger}$, of course, have been used. Equation (7) determines λ_q. Now (3), (5), and (7) are combined to obtain the interaction Hamiltonian between a test charge (at $\vec{r}$) and the plasmon modes:

$$H'(\vec{r}) = \textstyle\sum_{\vec{q}} M_q (a_{\vec{q}}\, e^{i\vec{q}\cdot\vec{r}} + a_{\vec{q}}^{\dagger} e^{-i\vec{q}\cdot\vec{r}}) , \tag{8}$$

with

$$M_q \equiv \left(\frac{2\pi e^2 \hbar \omega_P^2}{q^2 \Omega \omega_q} \right)^{1/2} . \tag{9}$$

The classical plasma frequency ω_P, given by

$$\omega_P^2 = 4\pi N e^2/m\Omega , \tag{10}$$

has been introduced and $\vec{q}$ has again been changed to $-\vec{q}$ in one of the terms while obtaining (8).

III. PLASMON FREQUENCY SPECTRUM

The plasmon dispersion relation ω_q, which should approach ω_P as $q \to 0$ and $\hbar q^2/2m$ as $q \to \infty$, will deviate from the true plasma frequency for $q > 0$. This is expected since the plasmon modes that have been defined must incorporate the oscillator strength of the one-electron excitations. ω_q is determined as follows: Consider a test charge of infinite mass located at the origin, $\vec{r} = 0$. The Fourier transform of its charge distribution is $\rho_{\vec{q}} = -e$. From the Maxwell equation $\mathrm{div}\vec{E} = 4\pi\rho$ the Fourier component of the electric field is $E_q = 4\pi e i/q\Omega$. In a vacuum the electrostatic energy associated with each Fourier component is

$$W_q = \Omega \left| E_q \right|^2 / 8\pi = 2\pi e^2/q^2\Omega . \tag{11}$$

However, in a dielectric medium having a dielectric constant ϵ_q, the electrostatic energy would be

$$W_q' = 2\pi e^2/q^2\Omega\epsilon_q . \tag{12}$$

Consequently, the change in energy arising from the interaction of the test charge with the dielectric is

$$W_q' - W_q = (2\pi e^2/q^2\Omega)(1/\epsilon_q - 1) . \tag{13}$$

Consider again the test charge (at $\vec{r} = 0$) interacting with the plasmon modes. The total Hamiltonian is

$$H = \textstyle\sum_{\vec{q}} [\hbar\omega_q a_{\vec{q}}^{\dagger} a_{\vec{q}} + M_q (a_{\vec{q}} + a_{\vec{q}}^{\dagger})] . \tag{14}$$

The first term is the plasmon Hamiltonian and the second is the interaction, from (8). The change in system energy attributable to the interaction is given by second-order perturbation theory. For

each mode $\vec{q}$

$$\Delta W_q = -M_q^2/\hbar\omega_q \ . \tag{15}$$

It is required that the two expressions (13) and (15) for the interaction energy be equivalent. With the help of (9) the plasmon frequency spectrum is obtained:

$$\omega_q^2 = \omega_P^2 \epsilon_q/(\epsilon_q - 1) \ . \tag{16}$$

Thus ω_q is determined once the (zero-frequency) dielectric function $\epsilon(q)$ is given. The derivation of (16) guarantees that the plasmon model will reproduce whatever ϵ_q deemed appropriate.

It is not possible to force the plasmon model to fit an *a priori* frequency-dependent dielectric function $\epsilon(q, \omega)$ since only a function of one variable ω_q is at one's disposal. Indeed, with the model completely specified, time-dependent perturbation theory could be used to derive from it a frequency dependence. The result would be unreliable at high frequency ($\omega \sim \omega_P$), however, since the spectral width of the true excitation spectrum is then important.

It is easy to verify that the frequency spectrum given by (16), and indicated by the dashed line in Fig. 1, has the correct limiting behavior. For $q \to 0$, one finds that $\epsilon_q \to \infty$; so $\omega_q \to \omega_P$. From Sec. IV it can be verified that

$$\epsilon_q - 1 \to 16me^2k_F^3/3\pi\hbar^2q^4 \quad \text{as} \quad q \to \infty \ .$$

With $N = \Omega k_F^3/3\pi^2$ and (10), it follows that $\omega_q \to \hbar q^2/2m$.

IV. DIELECTRIC FUNCTION

Unfortunately, the exact ϵ_q of an electron gas is unknown. In order to carry on, one must employ an approximate ϵ_q, which is derived by self-consistent perturbation theory including exchange and correlation potentials. The derivation is standard; it is repeated here in order to establish the notation. From perturbation theory, an electron gas subject to a (self-consistent) perturbing potential $V\cos\vec{q}\cdot\vec{r}$ will acquire a density variation $n = (N/\Omega) + \Delta n \cos\vec{q}\cdot\vec{r}$, where

$$\Delta n = -(3NV/2\Omega E_F) f(x) \ , \tag{17}$$

with $x \equiv q/2k_F$, $E_F \equiv \hbar^2k_F^2/2m$, and

$$f(x) \equiv \tfrac{1}{2} + [(1-x^2)/4x] \ln\left|(1+x)/(1-x)\right| \ . \tag{18}$$

From Poisson's equation, the Fourier coefficient of the electrostatic potential is

$$\varphi = 4\pi(\mu - e\Delta n)/q^2 \ , \tag{19}$$

where μ is the Fourier amplitude of an imposed charge distribution, causing the disturbance. The self-consistent potential is

$$V = -e\varphi + V_{xc} \ , \tag{20}$$

where V_{xc} is the exchange and correlation potential caused by Δn. This may be written as follows (if we approximate V_{xc} by a local potential):

$$V_{xc} \equiv -(e^2k_F\Omega/3\pi N) g(x) \Delta n \ . \tag{21}$$

$g(x)$ is a function that shall be specified later. The coefficient of (21) has been chosen so that if $g(x)$ were unity, V_{xc} would equal two-thirds of the oscillatory part of the potential given by the Slater $n^{1/3}$ exchange approximation.[4] (This is equivalent to the exchange term of the Kohn and Sham potential.[5])

Equations (17) and (19)–(21) constitute four linear equations relating the five variables Δn, V, φ, V_{xc}, and μ. From them the relation between φ and μ can be obtained:

$$\varphi \equiv 4\pi\mu/q^2\epsilon_q \ , \tag{22}$$

which defines the dielectric function

$$\epsilon_q = 1 + Q(x)/[1 - G(x)Q(x)] \ , \tag{23}$$

where

$$G(x) \equiv x^2 g(x)$$

and

$$Q(x) \equiv \frac{me^2}{\pi\hbar^2k_F} \frac{f(x)}{x^2} \ . \tag{24}$$

If V_{xc} had been neglected, $G(x)$ would be zero and (23) would become the Hartree (or Lindhard) dielectric function. The term involving $G(x)$ in the denominator of (23) is the positive feedback of exchange and correlation on dielectric response. The coefficient $C \equiv me^2/\pi\hbar^2k_F$ in (24) is a measure of the interaction strength. $C = 1$ corresponds to the electron density at which, in Hartree-Fock theory, the spin susceptibility diverges and the (long-wavelength) dielectric constant becomes negative.

Recent research on ϵ_q has been primarily a discussion of $G(x)$. The exact functional form of $G(x)$ is unknown, since that is equivalent to knowing the exchange and correlation potentials of a highly nonuniform electron gas. Although the exchange operator has been studied for such a case,[6] the correlation potential has not. Indeed, an ultimate goal of the plasmon model is to make such a study tractable.

Nevertheless important features in the behavior of $G(x)$ are known, for small x and large x. The small-x behavior is determined from the compressibility relation.[7] This relation may be easily derived as follows: Consider a positively charged plasma with a charge-to-mass ratio e/M and mass density nM. Its plasma frequency would be $(4\pi ne^2/M)^{1/2}$. If this plasma is imbedded in a dielectric medium with dielectric constant ϵ_q, the plasma frequency will be

$$\omega = \lim_{q \to 0} \left(\frac{4\pi ne^2}{M\epsilon_q}\right)^{1/2} \ . \tag{25}$$

If the dielectric medium happens to be an electron gas with $\epsilon_q \sim 1/q^2$ for small q, the plasma modes will in fact be longitudinal sound waves, so that

$$\omega = (\kappa n M)^{-1/2} q \ , \tag{26}$$

where κ is the compressibility. The equality of (25) and (26) leads to

$$\kappa = \lim_{q \to 0} \frac{q^2 \epsilon_q}{4\pi n^2 e^2} \ . \tag{27}$$

Note that M does not appear here. By letting $M \to \infty$, the positive plasma can be taken to have no internal energy of its own, thus κ is just the electron-gas compressibility. Equation (27) is the compressibility relation. From it we can derive the behavior of $G(x)$ as $x \to 0$.

The internal energy of an electron gas is

$$W = N(\tfrac{3}{5} E_F - 3e^2 k_F/4\pi + w_c) \ . \tag{28}$$

The first two terms are the kinetic and exchange energies, and w_c is the correlation energy per electron. By differentiating (28) appropriately the compressibility may be shown to be

$$\kappa = (3/2nE_F)[1 - (me^2/\pi\hbar^2 k_F)(1+\alpha)]^{-1} \ , \tag{29}$$

where

$$\alpha \equiv - \frac{4\pi}{3e^2}\left(\frac{dw_c}{dk_F} + \tfrac{1}{4} k_F \frac{d^2 w_c}{dk_F^2}\right) . \tag{30}$$

We now combine Eqs. (23), (27), and (29) and obtain $g(0) = 1 + \alpha$, so

$$G(x) \cong (1+\alpha) x^2 , \quad x \ll 1 \ . \tag{31}$$

Geldart and Vosko[8] were the first to emphasize that $G(x)$ should be chosen to satisfy the compressibility relation. It is of interest to observe that if this value $1+\alpha$ is used for $g(x)$ in Eq. (21), the coefficient of Δn is just $d\mu_{xc}/dn$, where μ_{xc} is the exchange and correlation contribution to the electron chemical potential. In other words, we have shown that if the Kohn and Sham (exchange *and* correlation) potential[5] is used in (21), the compressibility relation is satisfied exactly.

The numerical value of α can be computed from calculated values of w_c. In the metallic density regime $\alpha \cong 0.10$, there is little variation between the results obtained by different workers.[9] The fact that α is positive means that correlation effects enhance the dielectric response at long wavelengths. This result exemplifies a result obtained previously,[10] which seems paradoxical (to some): Exchange interactions enhance both paramagnetic and dielectric response; on the other hand, correlation effects suppress the former but enhance the latter.

The behavior of $G(x)$ for large x is related to the pair correlation function $p(\vec{r})$ at $\vec{r} = 0$[11] [provided $G(x)$ does not also depend on frequency],

$$G(\infty) = 1 - p(0) \ . \tag{32}$$

The exclusion principle causes the pair correlation function for parallel-spin electrons to be zero. At high electron densities, where Coulomb effects are small, $p(0) \cong \frac{1}{2}$ and arises entirely from electrons of antiparallel spin. At metallic densities, antiparallel-spin electrons are strongly repelled, resulting in much smaller values for $p(0)$. Accordingly, $0 < p(0) < \frac{1}{2}$ and $\frac{1}{2} < G(\infty) < 1$. The density dependence of $p(0)$ can be estimated from the wave function of an electron pair (in a singlet-spin state) while being scattered by a screened Coulomb potential. We have performed such a calculation[12] by a partial-wave phase-shift analysis and find, approximately,

$$p(0) \approx 32/(8+3r_s)^2 \ , \tag{33}$$

where r_s is the equivalent-sphere radius in Bohr units. At metallic densities, $2 < r_s < 6$, $p(0) \sim 0.1$, so $G(\infty) \sim 0.9$. The simplest algebraic function satisfying this and Eq. (31) is $1.1x^2/(1+1.22x^2)$. However, we find (Sec. VI) that this leads to correlation energies about 20% smaller than obtained by SSTL. Since the intent of this study is to find a simplified model that agrees in energy with the best prior work, we adopt for $G(x)$

$$G(x) = 1.1x^2/(1+10x^2+1.5x^4)^{1/2} \ . \tag{34}$$

This choice has the desired limiting behavior[13] for small and large x. The behavior at intermediate x, however, is more important in determining the correlation energy. The coefficient 10 of the x^2 term in (34) was determined by fitting the calculated correlation energy to that of SSTL at $r_s = 4$. Therefore, Eq. (34) is to some extent phenomenological (and model dependent). $G(x)$ does not rise as rapidly to its limiting value as the functions obtained by SSTL or Geldart and Taylor.[14] Although the $G(x)$ derived by SSTL does not have the correct limiting behavior, they showed that a rapid increase with x is necessary to prevent $p(\vec{r})$ from being negative near $\vec{r} = 0$.

V. ELECTRON-PLASMON INTERACTION

The interaction of a test charge with the plasmon coordinates, given by Eqs. (8) and (9), arises from the electrostatic potential associated with the plasmon charge fluctuations. For an electron the matrix element (9) must be corrected to include the exchange and correlation potential. This is obtained from Eq. (20) by substituting (19) and (21), observing that for plasmons $\mu \equiv 0$:

$$V = (4\pi e^2 \Delta n/q^2)[1 - G(x)] \ . \tag{35}$$

Consequently, the electron-plasmon interaction is given by Eq. (8), except that the matrix element M_q must be replaced by

$$M_q' = M_q[1 - G(x)] \ . \tag{36}$$

This (exchange and correlation) correction factor involves no further assumptions, since internal consistency requires that the $G(x)$ appearing here and in the dielectric function (23) be the same.

We believe that the test-charge-plasmon interaction [Eq. (8)] should also contain an extra factor $1-\gamma(x)$ analogous to (36), where $\gamma(x)$ arises from a (q-dependent) correlation potential for a test charge. To our knowledge this has not been studied. Thus refinement of the model in this way must be postponed.

VI. CORRELATION ENERGY $E_c(\vec{k})$

The one-electron energy $E(\vec{k})$ is the sum of three contributions:

$$E(\vec{k}) = \hbar^2 k^2/2m + E_x(\vec{k}) + E_c(\vec{k}) \ . \tag{37}$$

The second term is the exchange energy

$$E_x(\vec{k}) = \sum_{k' < k_F} \frac{-4\pi e^2}{\Omega |\vec{k}' - \vec{k}|^2} \ , \tag{38}$$

which can be readily evaluated. If we define $y \equiv k/k_F$,

$$E_x(\vec{k}) = -(2e^2 k_F/\pi) f(y) \ , \tag{39}$$

where $f(y)$ is the same function that appears in (18). The third term of (37) is the (k-dependent) correlation energy, which we can now calculate.

The one-electron correlation energy $E_c(\vec{k})$ is the total-system (interaction) energy with $\vec{k}$ occupied minus the energy with $\vec{k}$ empty. (Although we focus our attention on a single electron, we must account for the electrons in the plasma by means of the exclusion principle.) Accordingly,

$$E_c(\vec{k}) = \sum_{|\vec{k}-\vec{q}|>k_F} \frac{M_q^2[1-G(x)]^2}{E(\vec{k}) - E(\vec{k}-\vec{q}) - \hbar\omega_q} - \sum_{|\vec{k}+\vec{q}|<k_F} \frac{M_q^2[1-G(x)]^2}{E(\vec{k}+\vec{q}) - E(\vec{k}) - \hbar\omega_q} \ . \tag{40}$$

The first term is the second-order energy arising from the virtual emission and reabsorption of a plasmon $\vec{q}$, the electron at $\vec{k}$ being virtually excited to an empty state $\vec{k}' = \vec{k} - \vec{q}$ above the Fermi surface. The second term arises when the state $\vec{k}$ is empty. The hole at $\vec{k}$ is virtually excited to filled states $\vec{k}+\vec{q}$ below the Fermi surface.

The sums appearing in (40) are converted to integrations in the usual way. The two angular integrations that appear can be done analytically. $E_c(k)$ is then reduced to a single quadrature. With $x = q/2k_f$, $y \equiv k/k_F$,

$$E_c(k) = -\frac{me^4}{3\pi^2\hbar^2}\left(\int_0^{|1-y|/2} (1-G)^2 \frac{H\,dx}{xy} \times \ln\left| \frac{1 - Hxy - Hx^2}{1 + Hxy - Hx^2} \right| + \int_{|1-y|/2}^{|1+y|/2} (1-G)^2 \frac{H\,dx}{xy} \times \ln\left| \frac{(1+Hxy+Hx^2)(4-H+Hy^2)}{(1+Hxy-Hx^2)(4+H-Hy^2)} \right| \right.$$

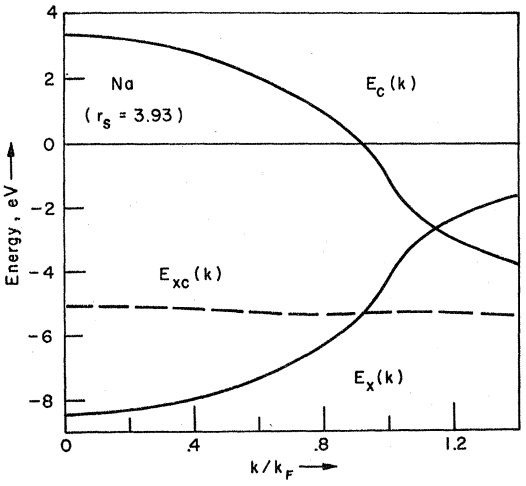

FIG. 2. Exchange energy $E_x(k)$ and correlation energy $E_c(k)$ and their sum $E_{xc}(k)$ for an electron gas with the density of Na. Both solid curves have logarithmically singular slopes at $k = k_F$, but the singularities cancel.

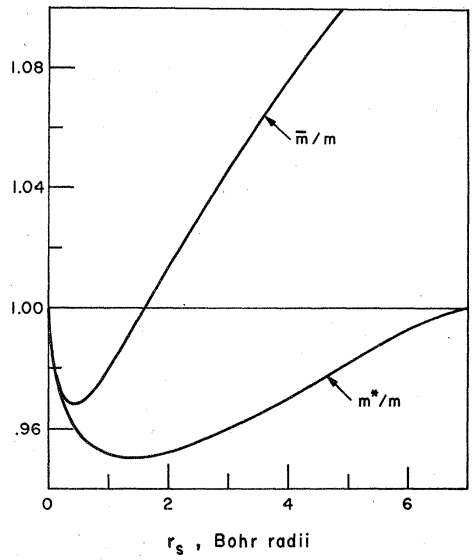

FIG. 3. Density-of-states effective mass m^* (at the Fermi surface) and the mean mass $\bar{m}$ (between $k=0$ and k_F) vs r_s, the radius of the equivalent sphere (in Bohr units).

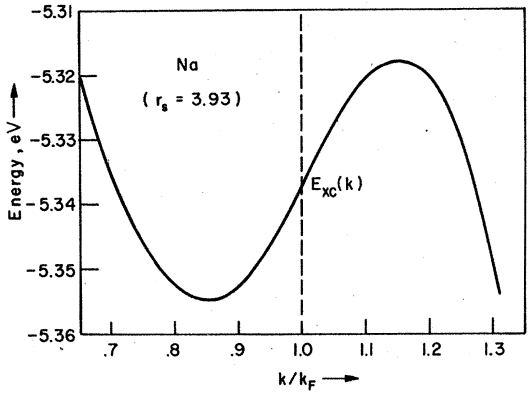

FIG. 4. Expanded plot of the exchange and correlation energy $E_{xc}(k)$ near the Fermi surface. This anomaly is responsible for most of the disparity between m^* and $\bar{m}$.

$$+\int_{|1+y|/2}^{\infty}(1-G)^2\frac{H\,dx}{xy}\ln\left|\frac{1+Hxy+Hx^2}{1-Hxy+Hx^2}\right|\Bigg)\,. \tag{41}$$

This expression is valid for $y \leq 1$. For $y > 1$, the argument in the logarithm of the first term (only) must be replaced by the argument appearing in the third term. The function $H(x)$ is

$$H(x) \equiv \left(\frac{3f(x)}{x^2+(me^2/\pi\hbar^2k_F)f(x)[1-G(x)]}\right)^{1/2}. \tag{42}$$

Numerical evaluation of (41) requires only a fraction of a second of computer time. In Fig. 2, $E_c(k)$ and $E_x(k)$ are shown for Na metal ($r_s = 3.93$, $k_F = 0.923\times10^8$ cm^{-1}). It should be noted that for most $k < k_F$, $E_c(k)$ is positive. This results from the fact that virtual transitions to small-k empty states are more effective than virtual transitions from the filled states. $E_c(k)$ falls precipitously near k_F, having a logarithmic singularity equal and opposite to a corresponding singularity in $E_x(k)$. That the cancellation of the singularities is exact can be quickly seen by rewriting (40) for small $q \equiv |\vec{k}' - \vec{k}|$. The energy denominators are then $\approx \hbar\omega_P$, thus

$$E_c(\vec{k}) \sim \sum_{k'>k_F}\frac{-2\pi e^2}{\Omega|\vec{k}'-\vec{k}|^2}+\sum_{k'<k_F}\frac{2\pi e^2}{\Omega|\vec{k}'-\vec{k}|^2}\,. \tag{43}$$

The exchange energy (38) represents an attraction (in k space) to filled states; the first term in (43) is an attraction to empty states, while the second term is a repulsion from filled states, each being one-half as strong as (38).

The sum $E_{xc}(k) \equiv E_x(k) + E_c(k)$ is almost independent of k, as shown by the dashed line in Fig. 2. Therefore, the many-body effective mass is close to unity. The density-of-states effective mass m^* (at k_F) is obtained from the slope of $E(k)$ and is shown in Fig. 3. The mean effective mass $\bar{m}$, defined by

$$\hbar^2k_F^2/2\bar{m} = E(k_F) - E(0)\,, \tag{44}$$

is also shown in Fig. 3. The deviation between m^* and $\bar{m}$ indicates the degree to which the many-body $E(k)$ is nonparabolic. The dependence of m^* on r_s that is found is very similar to that obtained by Hedin.[15] (The mass computed by Rice[16] resembles our result for $\bar{m}$.)

The one-electron energy $E_{xc}(k)$, attributable to interactions, undergoes a small oscillation near $k = k_F$. This is shown by the expanded plot in Fig. 4. The oscillation arises from the dynamic nature of the correlation energy. Had the recoil energy in the denominators of (40) been neglected, the oscillation would not have occurred. This can be understood in detail: The crude expression [Eq. (43)] fails as soon as q becomes appreciable. Inclusion of the recoil energy is necessary, and this moderates the k dependence of $E_c(k)$ relative to $E_x(k)$ near k_F. Most of the disparity between m^* and $\bar{m}$, shown in Fig. 3, is caused by this phenomenon. The maximum and minimum of $E_{xc}(k)$ are both about $0.15k_F$ from k_F. The kinetic energies at these points are ~1 eV above and below E_F. Since this energy difference is small compared to $\hbar\omega_P$, 6.05 eV, it is believed that the behavior given in Fig. 4 is real, and not an artifact of the model.

The total correlation energy W_c of an electron

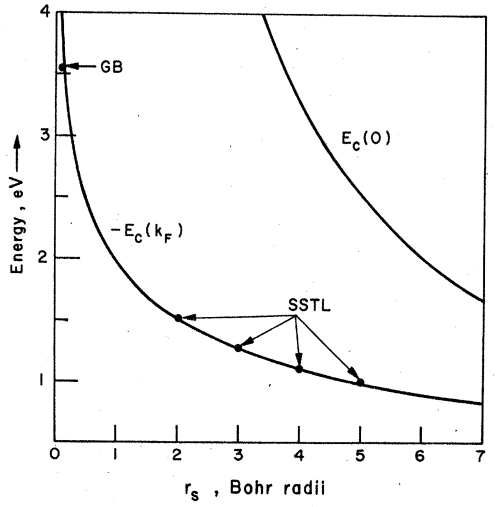

FIG. 5. Correlation contribution to the electron chemical potential $E_c(k_F)$ and the one-electron correlation energy at $k = 0$, both from Eq. (41). $E_c(0)$ is positive, indicating that when the electron at $k = 0$ is removed from the system virtual transitions to the (now) empty state are more effective than were transitions from $k = 0$ to states above k_F. The point GB was obtained from the Gell-Mann–Brueckner high-density limit; the other points were obtained from Singwi *et al.*, Ref. 1.

TABLE I. Calculated energy, mass, and occupation values for ideal electron assemblies having densities equal to those of six "free-electron" metals. ζ is the fractional number of electrons virtually excited above the Fermi surface. $E_x(0)$ is twice $E_x(k_F)$.

	Al	Li	Na	K	Rb	Cs
r_s	2.07	3.25	3.93	4.87	5.12	5.62
$\hbar\omega_P$(eV)	15.78	8.05	6.05	4.39	3.98	3.53
$\hbar^2k_F^2/2m$(eV)	11.65	4.75	3.24	2.12	1.86	1.58
$E_c(k_F)$(eV)	−1.48	−1.21	−1.11	−1.00	−0.97	−0.93
$E_x(k_F)$(eV)	−8.02	−5.12	−4.23	−3.42	−3.20	−2.96
$E_c(0)$(eV)	6.72	4.15	3.34	2.61	2.41	2.19
m^*/m	0.953	0.963	0.970	0.980	0.984	0.989
$\overline{m}/m$	1.016	1.054	1.074	1.099	1.107	1.117
$n(0)$	0.977	0.954	0.940	0.919	0.912	0.902
$n(k_{F-})$	0.863	0.798	0.764	0.721	0.707	0.689
$n(k_{F+})$	0.102	0.144	0.166	0.192	0.201	0.212
ζ	0.069	0.112	0.137	0.170	0.181	0.195

gas is

$$W_c = Nw_c \ , \tag{45}$$

where w_c is the correlation energy per electron, the quantity most workers compute. This can be compared with the results as follows: The correlation contribution to the electron chemical potential is

$$E_c(k_F) = \frac{dW_c}{dN} = w_c + N\frac{dw_c}{dN} \ . \tag{46}$$

Since $N \sim r_s^{-3}$, $dN/N = -3\,dr_s/r_s$. Accordingly, Eq. (46) becomes

$$E_c(k_F) = w_c - \tfrac{1}{3}\, r_s \frac{dw_c}{dr_s} \ , \tag{47}$$

a relation given by Seitz.[17] The second term of (47) is about 10% of the first and can be calculated from the published tables of $w_c(r_s)$.[9] In Fig. 5, we show $E_c(k_F)$ [from (41)] vs r_s. The points between $r_s = 2$ and 5 are those obtained from SSTL. The fit here is forced since, as indicated in Sec. IV, the adjustable parameter in the exchange and correlation function $G(x)$ [Eq. (34)] was fixed by requiring agreement at $r_s = 4$. The point labeled GB in the figure, at $r_s = 0.1$, was obtained from the Gell-Mann–Brueckner[18] high-density expansion. In the figure $E_c(0)$, the correlation energy of an electron at $k = 0$, is also shown.

Energy and mass values we have obtained are given in Table I for electron densities appropriate to six "free-electron" metals. (For real metals, contributions from band structure and electron-phonon interactions would have to be incorporated.)

VII. SCREENED-EXCHANGE AND COULOMB-HOLE POTENTIALS

Separation of $E(k)$ into three contributions – kinetic, exchange, and correlation – is (in the author's opinion) the most convenient division. However, other workers often separate $E_{xc}(k)$ into the sum of screened-exchange and Coulomb-hole potentials. This is merely a rearrangement of terms among Eqs. (38) and (40). The Coulomb-hole potential $E_{\rm CH}(k)$ is the first term of (40) with the sum extended over all $\vec{q}$, instead of just those $\vec{q}$ for which $|\vec{k} - \vec{q}| > k_F$:

$$E_{\rm CH}(k) \equiv -\sum_{\text{all } \vec{q}} \frac{M_q'^2}{\hbar\omega_q + \hbar\nu} \ , \tag{48}$$

where $\hbar\nu \equiv E(\vec{k}+\vec{q}) - E(\vec{k})$, and M_q' is (36). We subtract the extra terms we have added and combine them with the second term of (40) and all of (38) to obtain

$$E_{xs}(k) \equiv -\sum_{|\vec{k}+\vec{q}| < k_F} \left(\frac{4\pi e^2}{\Omega q^2} - \frac{M_q'^2}{\hbar\omega_q + \hbar\nu} - \frac{M_q'^2}{\hbar\omega_q - \hbar\nu} \right) \ . \tag{49}$$

This is the dynamically screened-exchange potential. By definition, $E_{xc}(k) = E_{xs}(k) + E_{\rm CH}(k)$. The k dependence of these potentials is shown in Fig. 6. It should be noted that the variation of $E_{\rm CH}(k)$ is larger than and opposite to that of screened exchange. Neglect of the Coulomb-hole potential can lead to serious error.[19]

The physical significance of the separate terms in (49) can be seen easily. First, neglect the recoil energy $\hbar\nu$. Then, from (9) and (36), each term of the sum can be written

$$V_{\vec{k}\vec{k}'} \approx -\frac{4\pi e^2}{\Omega q^2}\left(1 - \frac{\omega_P^2}{\omega_q^2}(1-G)^2\right) \ . \tag{50}$$

If the factor $(1-G)^2$ is now neglected and (16) is substituted,

$$V_{\vec{k}\vec{k}'} \sim -4\pi e^2/\Omega q^2 \epsilon_q \ , \tag{51}$$

which is a statically screened-exchange interaction. The terms contributing the screening are, of course, those arising from the virtual emission and

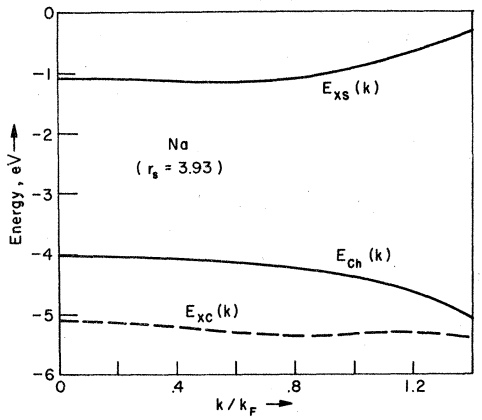

FIG. 6. Dynamically screened-exchange potential $E_{xs}(k)$ and the Coulomb-hole potential $E_{CH}(k)$. Their sum equals the sum $E_{xc}(k)$ of exchange and correlation potentials.

reabsorption of plasmons. The approximations just made are unjustified. However, the form of (51) suggests that we write each term of (49) exactly as

$$V_{\vec{k}\vec{k}'} \equiv -4\pi e^2/\Omega q^2 \epsilon^{ee}(q,\nu) \ , \tag{52}$$

which serves as a definition[20] of a frequency-dependent dielectric function for *electron-electron* interactions $\epsilon^{ee}(q,\nu)$. (One should remember that there are three distinct dielectric functions,[21] appropriate in turn to electron-electron, electron-test-charge, and test-charge–test-charge interactions, the latter being the "ordinary" dielectric function.) Neglect of $\hbar\nu$ involves approximation with a zero-frequency dielectric function; and neglect of $(1-G)^2$ involves substitution of a test-charge–test-charge dielectric function for an electron-electron one.

Separation of $E_{xc}(k)$ into screened-exchange and Coulomb-hole potentials does not seem useful unless some approximation such as (51) is to be employed. But then one should also neglect $\hbar\nu$ and $(1-G)^2$ in (48). $E_{CH}(k)$ would then be a constant, and the over-all k dependence of the resulting (approximate) $E_{xc}(k)$ would have the wrong sign.

VIII. LOCAL APPROXIMATION TO EXCHANGE AND CORRELATION

The exchange potential (39) has the values $-2e^2k_F/\pi$ at $k=0$, and $-e^2k_F/\pi$ at k_F. These are shown as functions of r_s by the upper and lower dashed lines in Fig. 7. The average of (39), obtained by integrating over the occupied states, is just the mean of these two limits, and is the Slater local-exchange approximation[4]

$$A_S = -3e^2(3n/8\pi)^{1/3} \ . \tag{53}$$

This is also shown in Fig. 7. The two solid lines in the figure are the sum of exchange and correlation potentials at $k=0$ and k_F. These curves cross at $r_s=1.6$, where $\bar{m}=1$ (see Fig. 3), and remain close together.

Many workers have employed approximate exchange potentials such as (53) in one-electron Schrödinger equations for atoms, molecules, and solids. In recent years, considerable success has resulted from use of αA_S as a local potential, where α is an adjustable scale factor. Kmetko[22] has found that the optimum α lies between $\frac{2}{3}$ and 1 for all atoms in the Periodic Table.

The narrow strip defined by the two solid lines in Fig. 7 lies between $\frac{2}{3}A_S = E_x(k_F)$ and A_S, but has a mean slope slightly smaller than $n^{1/3}$. A straight line connecting the points at $r_s=1.6$ and 10 has a slope corresponding to $n^{0.30}$. Accordingly, a local approximation to exchange *and* correlation potentials can be written

$$A_{xc} \approx -2.07(na_0^3)^{0.3} \text{ Ry} \ . \tag{54}$$

a_0 is the Bohr radius and, here, the electron density n is expressed in a_0^{-3} units. This simple expression represents the exchange and correlation potential rather well throughout a density range of 3 orders of magnitude. Since the contribution of E_{xc} to the bandwidth is so small, (54) is also a good approximation to the Kohn and Sham potential $E_{xc}(k_F)$.

The trustworthiness of local approximations to exchange and correlation remains an open question,

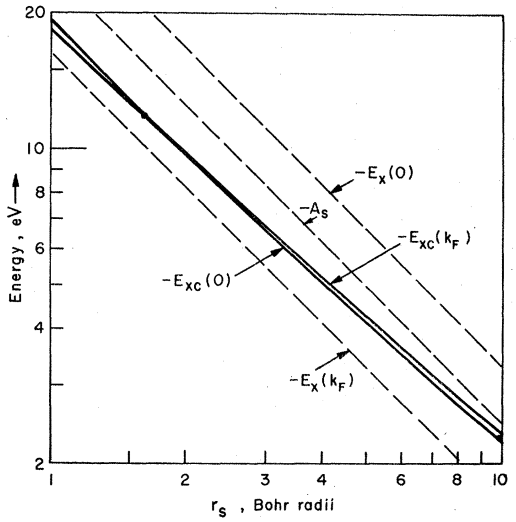

FIG. 7. Upper and lower dashed lines are the exchange potentials for an electron at $k=0$ and k_F. The average potential (for occupied states) is A_S. The two solid lines are the exchange- and correlation-potential sums at $k=0$ and k_F. They cross at $r_s=1.6$. A straight line through this point and the one at $r_s=10$ corresponds to $-2.07 \times (na_0^3)^{0.3}$ Ry.

especially since the nonlocal effects of exchange have been shown to be quite pathological.[6] Although the extreme behavior of the exchange operator may be well compensated for by correlation, the fact that exchange is kinematic in origin, whereas correlation is dynamic, leaves room for uncertainty. This is of particular concern for energy-band calculations where energy gaps and Fermi-surface shapes are to be determined. The oscillation in $E_{xc}(k)$ near k_F (Fig. 4) is an example of imperfect compensation in a homogeneous case.

IX. MOMENTUM DISTRIBUTION $n(k)$

For the ground state of a noninteracting electron gas $n(k)=1$, $k<k_F$ and $n(k)=0$, $k>k_F$. Coulomb interactions cause the electrons to experience virtual excitation to (otherwise) empty states above k_F. Consequently, $n(k)$, the expectation value of the occupation number (for the pure-momentum states) will be <1, $k<k_F$ and >0, $k>k_F$. The theoretical momentum distribution $n(k)$ is of considerable interest since it can be directly measured by Compton scattering of x rays.[23] In principle, such experiments can provide a direct and detailed test of many-body theory.

Consider a state $\vec{k}$ below k_F. If the electron in this state is excited through virtual emission of a plasmon $\vec{q}$, which can occur only if $|\vec{k}-\vec{q}|>k_F$, the fractional occupation of the state $\vec{k}$ is reduced by the normalization factor

$$\left(1+\frac{M_q'^2}{(\hbar\omega_q+\hbar\nu)^2}\right)^{-1}, \tag{55}$$

the notation being the same as in (48). Each allowed virtual excitation will contribute a similar factor, so

$$n(\vec{k})=\prod_{\vec{q}}\left(1+\frac{M_q'^2}{(\hbar\omega_q+\hbar\nu)^2}\right)^{-1}. \tag{56}$$

Taking the logarithm of this expression, one observes that each term, $\ln(1+\delta)$, can be replaced by δ since $\delta\sim 1/N$. Accordingly,

$$\ln[n(\vec{k})]=-\sum_{|k-q|>k_F}\frac{M_q'^2}{(\hbar\omega_q+\hbar\nu)^2}. \tag{57}$$

As in Sec. VI, the indicated summation can be performed up to a single quadrature. With $x\equiv q/2k_F$ and $y\equiv k/k_F<1$ one obtains

$$\ln[n(k)]=-\frac{m^2e^4}{6\pi^2\hbar^4k_F^2}\times\left(\int_{(1-y)/2}^{(1+y)/2}\frac{H^3(1-G)^2(4xy+4x^2+y^2-1)\,dx}{(1+Hxy+Hx^2)(4+H-Hy^2)xy}+\int_{(1+y)/2}^{\infty}\frac{2H^3(1-G)^2\,dx}{(1+Hx^2)^2-(Hxy)^2}\right). \tag{58}$$

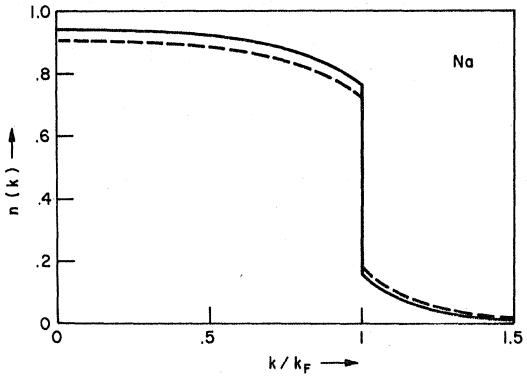

FIG. 8. Momentum distribution for an interacting electron gas having the density of Na. Dashed curve is obtained if exchange and correlation corrections to the matrix elements causing virtual excitations are omitted.

$G(x)$ and $H(x)$ are given by (34) and (42), as before. Similarly, for $k>k_F$,

$$\ln[1-n(k)]=-\frac{m^2e^4}{6\pi^2\hbar^4k_F^2}\times\int_{(y-1)/2}^{(y+1)/2}\frac{H^3(1-G)^2(4xy-4x^2-y^2+1)\,dx}{(1+Hxy-Hx^2)(4-H+Hy^2)xy}. \tag{59}$$

$n(k)$ is shown in Fig. 8 for an electron gas having a density equivalent to that of Na. The discontinuity at k_F is ~ 0.60 (compared to unity for the noninteracting gas). The dashed curve in Fig. 8 is the $n(k)$ obtained if the factor $(1-G)^2$ is deleted from the integrands of (58) and (59). The result, which neglects exchange and correlation contributions to the matrix elements, agrees with the work of Daniel and Vosko,[24] Corrections for exchange and correlation have also been studied by Geldart, Houghton, and Vosko[25] and are comparable to the differences shown in Fig. 8.

The fractional number ζ of electrons excited above the Fermi surface is given by

$$\zeta=\int_0^{k_F}\frac{[1-n(k)]3k^2\,dk}{k_F^3}. \tag{60}$$

For the electron density of Na, one obtains $\zeta=0.137$, a relatively small number considering that the dimensionless interaction strength $C=me^2/\pi\hbar^2k_F$ is 0.65. The smallness of ζ can be attributed to the exclusion principle which inhibits the effects of the interaction. One should appreciate that the validity of any theory at metallic densities depends on the smallness of ζ. The variation of ζ with r_s and several limiting values of $n(k)$ are shown in Fig. 9. Tabulated values appropriate to the densities of several metals are given in Table I.

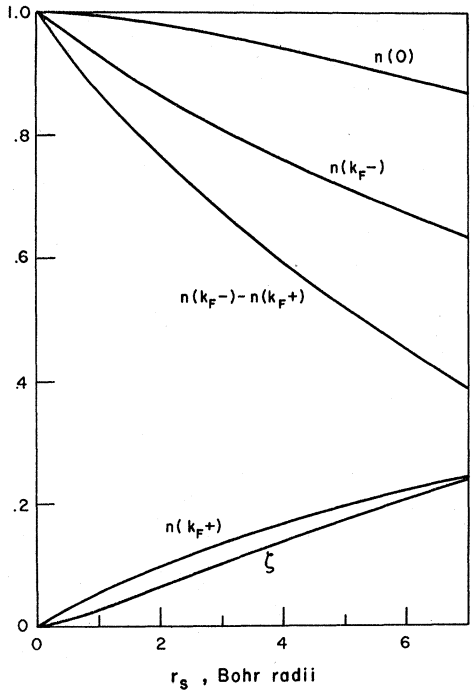

FIG. 9. Variation of ζ, the number of virtually excited electrons, and limiting points of $n(k)$ with r_s.

The momentum distribution computed here cannot be compared with that obtaining in real metals until band-structure contributions are incorporated. There are two important effects. Conduction-electron wave functions are linear combinations of plane waves:

$$\psi_{\vec{k}} = e^{i\vec{k}\cdot\vec{r}} \sum_{\vec{G}} \alpha_{\vec{G}}(\vec{k}) e^{2\pi i \vec{G}\cdot\vec{r}} , \qquad (61)$$

where $\{\vec{G}\}$ are the reciprocal-lattice vectors. The higher-momentum components, the terms in (61) with $\vec{G} \neq 0$, contribute directly to the momentum distribution, and the $\vec{G} = 0$ term $\alpha_0(\vec{k})^2$ is correspondingly depleted. Finally, the matrix elements of the correlation excitations will on the average be enhanced[10] by the modulation occurring in $\psi_{\vec{k}}$. Not only will individual matrix elements M_q be altered, but new ones, for which $\vec{k}' = \vec{k} - \vec{q} + 2\pi\vec{G}$, will occur. The simple model given here provides a method which may allow such effects to be calculated.

X. CONCLUSION

We have shown that the plasmon model provides an easy method for calculating the effects of correlation on one-electron energy spectra. The dynamic origin of correlation leads to an anomaly in $E_{xc}(k)$ near k_F that is responsible for a large disparity between m^* and $\bar{m}$. On the other hand, the near (over-all) cancellation of $E_x(k)$ and $E_c(k)$, in their k dependence, allows a specific local approximation to the exchange and correlation potential. The dangers involved in employing screened-exchange approximations were made explicit.

The momentum distribution $n(k)$, including exchange and correlation contributions to the matrix elements, was computed as a function of r_s. The fraction ζ of electrons excited above k_F was found to be smaller by about a factor of 5 than the dimensionless interaction constant. This leads one to believe that (properly self-consistent) calculations of many-body effects in the metallic regime are reasonably accurate.

The plasmon model appears to be a tractable method for investigating correlation effects in inhomogeneous problems. However, it may need some generalization for problems involving spin polarization.

[1]K. S. Singwi, A. Sjölander, M. P. Tosi, and R. H. Land, Phys. Rev. B 1, 1044 (1970).

[2]R. A. Ferrell, Phys. Rev. 107, 450 (1957) (Sec. V).

[3]P. Nozières and D. Pines, Phys. Rev. 109, 741 (1958).

[4]J. C. Slater, Phys. Rev. 81, 385 (1951).

[5]W. Kohn and L. J. Sham, Phys. Rev. 140, A1133 (1965).

[6]A. W. Overhauser, Phys. Rev. B 2, 874 (1970).

[7]D. Pines and P. Nozières, *Theory of Quantum Liquids* (Benjamin, New York, 1966), p. 105.

[8]D. J. W. Geldart and S. H. Vosko, Can. J. Phys. 44, 2137 (1966).

[9]α can be derived from the data given in Ref. 1, Table I, or Fig. 4. In the figure, the Hartree-Fock $1/\kappa$ corresponds to a straight line intersecting the abscissa at $r_s = 6.03$.

[10]A. W. Overhauser, Phys. Rev. 167, 691 (1968).

[11]R. W. Shaw, Jr., J. Phys. C 3, 1140 (1970).

[12]A. W. Overhauser, Ph. D. thesis, University of California, Berkeley, 1951, Chap. VIII (unpublished).

[13]The dielectric function of J. Hubbard [Proc. Roy. Soc. (London) A243, 336 (1957)] corresponds in our notation to $G(x) = 2x^2/(1+4x^2)$. The compressibility relation is violated seriously, so much so that the long-wavelength ϵ_q of all the alkali metals would be negative.

[14]D. J. W. Geldart and R. Taylor, Can. J. Phys. 48, 167 (1970).

[15]L. Hedin, Phys. Rev. 139, A796 (1965) (Fig. 12).

[16]T. M. Rice, Ann. Phys. (N. Y.) 31, 100 (1965).

[17]F. Seitz, *The Modern Theory of Solids* (McGraw-Hill, New York, 1940), p. 344.

[18]M. Gell-Mann and K. A. Brueckner, Phys. Rev. 106, 364 (1957).

[19]Geldart and Vosko, Ref. 14, p. 2144, have pointed out several examples where this has occurred, even in calculations of homogeneous properties.

[20]Since our model makes no provision for dissipation, this must be interpreted as a definition of the real part of $1/\epsilon(q, \nu)$.

[21]L. Kleinman, Phys. Rev. 172, 383 (1968).

[22]E. A. Kmetko, Phys. Rev. A 1, 37 (1970).

[23]W. C. Phillips and R. J. Weiss, Phys. Rev. 171,

790 (1968).
[24]E. Daniel and S. H. Vosko, Phys. Rev. 120, 2041 (1960).
[25]D. J. W. Geldart, A. Houghton, and S. H. Vosko, Can. J. Phys. 42, 1938 (1964).

PHYSICAL REVIEW B VOLUME 3, NUMBER 6 15 MARCH 1971

Interband Absorption and the Optical Properties of Polyvalent Metals*

N. W. Ashcroft and K. Sturm
Laboratory of Atomic and Solid State Physics, Cornell University, Ithaca, New York 14850
(Received 21 May 1970)

Excitation of electrons between parallel or near-parallel one-electron bands in simple polyvalent metals constitutes a major source of the observed optical absorption. Much of the effect can be accounted for in a straightforward calculation of both real and imaginary parts of the conductivity, which does not require the constant-matrix-element assumption. In many cases, the magnitude and rounding of the absorption edges (singular in the absence of scattering) are quite sensitive to the phenomenological relaxation times (and hence to temperature) and to surface scattering. The sum rule for the (transverse) optical conductivity is related to the Fourier components of the weak periodic potential, and an expression is derived for the optical mass. The theory has been applied to study the optical properties of Al.

I. INTRODUCTION

Structure in the observed optical absorption from metals is normally related to singular behavior in the joint density of states associated with the single-particle bands. In polyvalent metals it is often found that by plotting the bands along certain directions in $\vec{k}$ space, a pair of them may be substantially parallel. This is the situation, for example, in Al,[1-4] and Ehrenreich *et al.*[5] observed that absorption edges of notable strength would go hand in hand with a parallel-band spectrum. The behavior of the absorption and the nature of the edge was partially analyzed for photon energies in the neighborhood of the threshold by Harrison,[6] who predicted (on the basis of independently calculated pseudopotentials) the position of absorption edges for a number of metals.

For energies sufficiently close to the edge, the oscillator strength required in Ref. 6 can be taken as effectively constant. In a more recent numerical calculation, Dresselhaus *et al.*[7] incorporated (among other things) the explicit $\vec{k}$ dependence of the oscillator strengths and obtained reasonable agreement with new data on Al reported in the same paper. Again, these data display prominent edges which reflect the presence of parallel bands (as noted in Ref. 6).

It is the purpose of this paper to demonstrate that the dominant features in the absorption actually follow quite straightforwardly from a simple weak-potential (or pseudopotential) representation of the important bands. We treat two cases: The first, in which scattering is assumed absent, is outlined in Sec. II and essentially reproduces for parallel-band absorption the results of Golovashkin *et al.*[8] We extend the analysis and derive an expression for the absorption which may be of interest at higher energies. To account for the broadening of the single-particle bands, we use a relaxation-time approximation result for the frequency-dependent conductivity (Sec. III). It is easy to show that the height of the edge is sensitive in this model to the choice of relaxation time τ, an observation which may account in some measure for the reported variations in the experimental values for $\sigma(\omega)$. For metals possessing one or more *small* band gaps ($\sim$few $\hbar/\tau$), it is apparent from the analysis that the broadening may extend to low energies, thereby adding to what is normally considered to be Drude, or intraband, scattering. The theory that follows is illustrated by explicitly evaluating both the real and imaginary parts of the optical conductivity $\sigma(\omega)$ for the cubic metal Al. (Generalization to noncubic systems is straightforward.) Determination of the surface and volume plasma frequency for Al from the imaginary part of the conductivity reveals good agreement with the results from electron energy-loss experiments. Finally, the contribution of the interband absorption to the sum rule for $\mathrm{Re}\sigma(\omega)$ is shown to lead to a simple relation involving the Fourier components (U_K) of the weak single-particle potential. It is also possible to derive an explicit relation for the optical effective mass in terms of the U_K's, whose compatibility with the requirements of the sum rule on the total (intraband and interband) absorption is easily demonstrated.